Environmental Modeling and Assessment (2006) **11:** 101–114
DOI: 10.1007/s10666-006-9047-5

Coupling climate and economic models in a cost-benefit framework: A convex optimisation approach

L. Drouet[a,*], N. R. Edwards[b] and A. Haurie[a]

[a] *Logilab-HEC, University of Geneva, Geneva, Switzerland*
E-mail: Laurent.drouet@hec.unige.ch; alain.haurie@hec.unige.ch
[b] *Climate and Environmental Physics, University of Bern, Bern, Switzerland*
E-mail: n.r.edwards@open.ac.uk

In this paper, we present a general method, based on a convex optimisation technique, that facilitates the coupling of climate and economic models in a cost-benefit framework. As a demonstration of the method, we couple an economic growth model à la Ramsey adapted from DICE-99 with an efficient intermediate complexity climate model, C-GOLDSTEIN, which has highly simplified physics, but fully 3-D ocean dynamics. As in DICE-99, we assume that an economic cost is associated with global temperature change: this change is obtained from the climate model, which is driven by the GHG concentrations computed from the economic growth path. The work extends a previous paper in which these models were coupled in cost-effectiveness mode. Here we consider the more intricate cost-benefit coupling in which the climate impact is not fixed *a priori*. We implement the coupled model using an oracle-based optimisation technique. Each model is contained in an oracle, which supplies model output and information on its sensitivity to a master program. The algorithm Proximal-ACCPM guarantees the convergence of the procedure under sufficient convexity assumptions. Our results demonstrate the possibility of a consistent, cost-benefit, climate-damage optimisation analysis with a 3-D climate model.

Keywords: integrated assessment model, coupling, economy, climate, convex optimization, oracle

1. Introduction

The aim of this paper is to present a convex optimisation method to couple climate and economic models within an Integrated Assessment Model (IAM) framework. IAMs have been introduced as processes for combining and communicating knowledge from diverse scientific disciplines [21]. The two principal objectives for IAMs have been defined as (1) adding value compared to an assessment model based on a single discipline and (2) providing comprehensive information to policy makers [19]. Schneider [22] distinguishes three modelling approaches of IAMs: policy evaluation models (such as the IMAGE model [1]), policy optimisation models (the DICE [18] and MERGE [16] models) and policy guidance models (the ICLIPS model [23]). Policy guidance models typically solve a cost-effectiveness problem within certain bounds on allowed impact. This paper focuses on policy optimisation models. Such models identify optimal policies, given a set of targets, with the help of optimisation techniques [13] and thus effectively solve a cost-benefit problem. The cost-benefit approach arises naturally from the economic formulation of the climate change issue and has obvious advantages of simplicity of interpretation and communication. On the other hand, there are major difficulties associated with the practical application of such an analysis, as summarized by Dowlatabadi [4]: it assumes that all damages and risks can be valued in monetary terms, and that the relevant actors could agree on such a valuation; it assumes that all costs are marginal; and it assumes the possibility of redistribution of wealth between those who benefit and those who suffer the costs. Nevertheless, demonstration of the feasibility of such a calculation still represents progress in exposing the relevant issues.

The overwhelming bulk of climate modelling effort is directed towards relatively highly detailed Atmosphere and Ocean General Circulation Models (AOGCMs), which directly simulate many of the key processes operating in the climate system [11]. Unfortunately, because of constraints imposed by available algorithms, computer memory requirements and, most of all, processing time required to run these models as well as the difficulties associated with translating and porting large numerical codes, such highly detailed AOGCMs cannot be directly integrated in existing IAM frameworks. According to Nordhaus and Boyer [18], inclusion of GCMs in an optimisation model such as DICE-99 is infeasible. Technically, C-GOLDSTEIN is a GCM, at least for the ocean, although the term GCM is frequently understood to refer exclusively to higher-resolution models. In this paper, therefore, we present a framework that allows a representation of climate dynamics in IAMs that includes more detailed dynamics than in previous studies, but still permits the calculation of optimal policies.

The ultimate facility would be an all-encompassing model with an economic sub-model, a climate sub-model and a numerical module, which controls the optimisation procedure, without strong modifications inside the models. A first approach has been described by Jansenn et al. [13], where he couples the economic part of DICE with a climate representation from the IMAGE model [1]. He

* Corresponding author.

proposes a heuristic method to find a local optimal solution. More recently, Leimbach and Jaeger [15] have explored a modular approach. In their coupled model, they reuse the economic model from ICLIPS, named ICE-MODE, and couple it successively with two climate models: one from ICLIPS with a simple representation of climate, and the other, the MAGICC model [26], which is essentially a model emulator that reproduces the behaviour of the IPCC model studies. A meta-optimizer module executes the optimisation procedure, and a job control module governs the communication between the other modules. The climate subcomponent in all these cases is highly simplified, in no case including a fluid dynamical model of the ocean or atmosphere.

In this research, we couple an economic growth model, which is an adaptation of the DICE-99 model of Nordhaus [17, 18], with the efficient climate model C-GOLDSTEIN [6]. We refer to the coupled model as GOLDICE. In [5], a coupling of these two models in a cost-effectiveness manner is described, where the median of the temperature change distribution is not allowed to exceed a threshold of 2.5°C at the end of the time horizon. The constraint on temperature increase could be criticized because it was not endogenously related to damage cost in the economic model. Moreover, the temperature change constraint is only active at the end of the simulation. Here, we use a similar approach but in a cost-benefit framework. The coupling is implemented through the use of a convex programming method, called the Proximal Analytic Center Cutting Plane Method (Proximal-ACCPM) [7]. At each iteration, Proximal-ACCPM supplies a query point, and an "oracle" provides the model's sensitivity at this point. An "oracle" is simply a structure built around the model, which has the capacity to ask the model two questions: "What is the value of a given model output (e.g. the value of the objective function) at a given point?" and "What is the gradient of the output with respect to certain given inputs at this point?." Under the hypothesis of dealing with convex models, Proximal-ACCPM guarantees the convergence of the coupling. This algorithm has been used in [3] to couple a technico-economic model (MARKAL Geneva) with an ozone model to study local air pollution and its technology response.

Currently, most of these IAMs are written in a single metalanguage, and the different parts that describe the respective phenomena are strongly linked to form a compact model. Thus, it is not easy to extend an existing IAM without interfering with the existing code. Our approach offers a modular-oriented framework appropriate to a new generation of IAMs, the Community Integrated Assessment Models (CIAMs), the concept of which is to combine components and knowledge from different modelling groups. CIAMs should be built to be more expansible, transparent, applicable and credible than more tightly linked IAMs [12]. IAMs bring together climate models, socio-economic models, models of technological change, policy models, transport models and models of social behaviour and decision making. Collaborative IAMs add a cooperative approach to integrated assessment by involving several institutes, which either have already built IAMs and can offer an existing module or are specialist in a domain, e.g. an ocean representation for an oceanographic institute. The first implementation of a collaborative IAM has been initiated by a European group including the UK Tyndall Center [24] and is referred to as CIAM^n. The related SoftIAM project provides a flexible implementation framework, which enables different modules to be interconnected using common XML specifications. The procedure we describe in this paper could be relevant in CIAMs when optimisation and simulation models are linked.

The paper is organized as follows. In Section 2, we describe the modular structure of the model; in Section 3, we describe the reduced-order coupling problem and the Proximal-ACCPM algorithm, which realizes the coupling; in Section 4, we present the implementation and some numerical results. Section 5 concludes and proposes a future research agenda.

2. Methodology

The GOLDICE approach is summarized in Figure 1, which shows the two main parts or "oracles" involved. Communication between the modules is indicated by the arrows in the figure. The two coupling variables are the carbon emissions and the temperature change. The sharing of these variables forces a consistency between the two oracles. The climate oracle is composed of two independent modules: carbon cycle and C-GOLDSTEIN. Inside the carbon-cycle module (see Section 2.2), carbon concentration accumulations are calculated with the DICE-99 equations. These equations represent the carbon exchanges between three reservoirs (the atmosphere, the mixing reservoir in the upper oceans and the biosphere, and the deep oceans). The climate model C-GOLDSTEIN, also described in Section 2.2, is a fast, coupled climate model. C-GOLDSTEIN computes the temperature changes for a given carbon concentration pathway. The economy oracle, detailed in the next section, maximizes the global welfare and calculates the induced anthropogenic carbon emissions. For cost-benefit purposes, a damage function computes a loss in production due to climate change. The economy equations, the carbon-cycle system and the damage function come from the DICE-99 model. The following sections describe the content of the different modules.

2.1. The economy model

The equations of the economy model are taken from the DICE-99 model of Nordhaus and Boyer [18]. They describe both the economic dynamics and the damage function. DICE-99 is a global model that provides greenhouses gas emissions derived from a moderately complex, globally aggregated economic model, driven by population

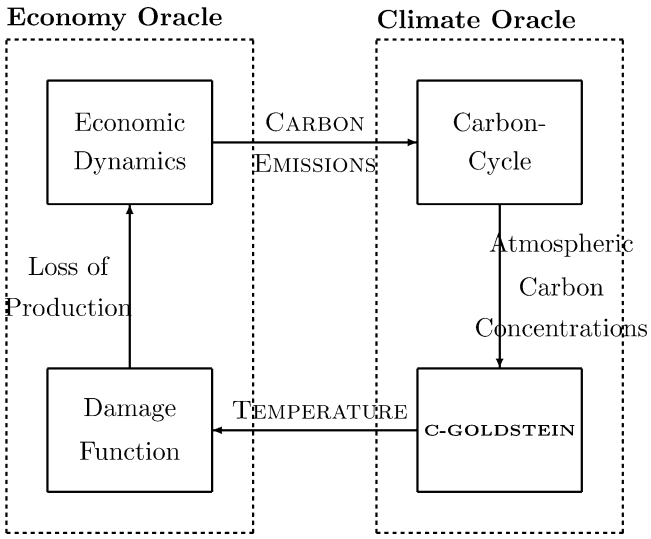

Figure 1. GOLDICE framework.

growth and labour productivity. Damage to the economy is represented by a simple cost feedback. The economic equilibrium is obtained by solving for optimal economic growth "à la Ramsey," over a planning horizon $\mathcal{T} = \{0, 1, \ldots, t_{\max}\}$. The equations of the model are listed below; note that t represents the *integer* value of the time index, not the real value of time, which is discretized in 10-year steps. The model maximizes the sum of the discounted welfare (or utility of consumption) $W(c(t), L(t))$ over all the periods as shown in Eqs. (1) and (2). When $\alpha = 1$, the utility function takes the form $L\log(c)$:

$$\max \sum_{t\in\mathcal{T}} \rho(t) W(c(t), L(t)) \tag{1}$$

$$\text{s.t.} \quad W(c(t), L(t)) = L(t)\frac{c(t)^{1-\alpha} - 1}{1-\alpha}, \ t \in \mathcal{T} \tag{2}$$

$$c(t) = \frac{C(t)}{L(t)}, \ t \in \mathcal{T}. \tag{3}$$

The per-capita value of consumption, c, is defined in Eq. (3). Eqs. (4)–(10) compute the exogenous parameters of the model. The discount rate ρ is decreasing over time. This is a controversial issue discussed in [10]. The population, represented by the labour L, and the technical progress A are growing and stabilizing toward an asymptotic value. The deforestation ET decreases to zero over time.

$$r(t) = r_1 e^{-d\times r_2(t-1)}, \ t \in \mathcal{T} - \{0\} \tag{4}$$

$$\rho(t+1) = \frac{\rho(t)}{1 + r(t)^d}, \ t \in \mathcal{T} - \{t_{\max}\} \tag{5}$$

$$L(t) = L_0 e^{g_L(t)}, \ t \in \mathcal{T} \tag{6}$$

$$g_L(t) = g_{L_0}(1 - e^{-g_\delta(t-1)}), \ t \in \mathcal{T} - \{0\} \tag{7}$$

$$A(t+1) = \frac{A(t)}{1 - g_A(t)}, \ t \in \mathcal{T} - \{t_{\max}\} \tag{8}$$

$$g_A(t) = g_{A_0} e^{-g_\delta(t-1)}, \ t \in \mathcal{T} - \{0\} \tag{9}$$

$$ET(t) = ET_0 e^{-g_{ET}(t-1)}, \ t \in \mathcal{T} - \{0\}. \tag{10}$$

Output Q is calculated by a typical Cobb–Douglas production function in Eq. (11). The production factors are labour L, capital K and exogenous technical change A. The abatement effort μ ($\in [0; 1]$) induces a loss of production. An important part of this equation is the damage function D, Eq. (12), which also affects production. Impacts of climate change on the economy are not easy to quantify and monetize, even though literature in this field is extensive. Impacts vary among sectors and countries depending on local or global climate change. Climatic factors such as the frequencies of storms and floods may have more influence on economic activity than average temperature. However, mean temperature is used in the damage function here as an index of climate change, subsuming more complex interactions between climate and economic variables. A whole chapter of discussion on the calibration of the damage function can be found in [18].

Emissions E are a function of the carbon intensity of the production technologies σ and the abatement effort μ. Deforestation ET adds supplementary emissions.

$$Q(t) = A(t)L(t)^{1-\gamma}K(t)^{\gamma}(1 - b_1\mu(t)^{b_2})D(T(t)), \ t \in \mathcal{T} \tag{11}$$

$$D(t) = (1 + a_1 T(t) + a_2 T(t)^2)^{-1}, \ t \in \mathcal{T} \tag{12}$$

$$E(t) = d\sigma(t)(1 - \mu(t))A(t)L(t)^{1-\gamma}K(t)^{\gamma} + ET(t), \quad t \in \mathcal{T}. \tag{13}$$

Eq. (14) represents the relation between production Q, consumption C and investment I. The interperiodic relation between investment I and capital K is described in Eq. (15).

$$Q(t) = C(t) + I(t), \ t \in \mathcal{T} \tag{14}$$

$$K(t+1) = d \times I(t) + (1-\delta)^d K(t),\ t \in \mathcal{T} \tag{15}$$

Finally, Eqs. (16) and (17) control the value of the coupling variables E and T inside the model. These two equations are very important for the consistency of the model. At the optimum, the dual variables associated with these equations give the sensitivity of the model with respect to the bounds E_{up} and T_{lo}.

$$E(t) \le E_{up}(t),\ t \in \mathcal{T} - \{0\} \tag{16}$$

$$T(t) \ge T_{lo}(t),\ t \in \mathcal{T} \tag{17}$$

The parameter values are shown in Table 1. In comparison with DICE-99, equations related to the temperature change and the induced forcing have been removed. These equations are replaced with constraint (17), which imposes that the temperature change $T(t)$, included in the damage function, is at least equal to the temperature change bound $T_{lo}(t)$. The upper bound on emissions is the other constraint (16) introduced in the economic model. The value $E_{up}(t)$ is used to compute atmospheric carbon concentrations that will drive C-GOLDSTEIN for the computation of temperature change $T_{lo}(t)$. The generation of $E_{up}(t)$ and $T_{lo}(t)$ is explained in detail in the next section.

In the coupled model, we use a compact form of the economic model, which will serve to define a "reduced-order" optimisation problem where a value function $U(E_{up}, T_{lo})$ is obtained as the maximized discounted utility subject to the constraints on emissions and temperature changes. This compact-form problem is summarized as follows

$$U(\tilde{E}_{up}, \tilde{T}_{lo}) = \max f(\tilde{E}, \tilde{T}, \upsilon) \tag{18a}$$

$$\text{s.t.}\quad \psi(\tilde{E}, \tilde{T}, \upsilon) \le 0, \tag{18b}$$

$$\tilde{E} \le \tilde{E}_{up}, \tag{18c}$$

$$\tilde{T} \ge \tilde{T}_{lo} \tag{18d}$$

where f represents the discounted utility summed over the planning horizon [Eq. (1)], $\tilde{E} = (E(t) : t \in \mathcal{T} - \{t_{\max}\})$ and $\tilde{T} = (T(t) : t \in \mathcal{T})$ are the emissions and temperature change schedules, respectively. $\tilde{E}_{up}$ and $\tilde{T}_{lo}$ are the upper- and lower-bound schedules for $\tilde{E}$ and $\tilde{T}$, respectively. The vector υ summarizes all the other economic variables implicated in the model. Eqs. (2)–(15) are summarized in the global Eq. (18b). The last two Eqs. (18c) and (18d) correspond to Eqs. (16) and (17).

2.2. The climate model

C-GOLDSTEIN is a flexible geometry, efficient, frictional geostrophic, 3-D global ocean model with eddy-induced and isopycnal interior mixing coupled with a single-layer, "Energy and Moisture Balance" atmosphere and a dynamic and thermodynamic sea-ice component. With an integration speed of 1,000 or 2,000 years per hour on a modern PC, it is an order of magnitude less efficient than the Bern 2.5-D model, but 3 or 4 orders of magnitude faster than conventional, high-resolution models such as HadCM3 [8] and 1 or 2 orders of magnitude faster than other intermediate complexity models such as the UVic model [25]. This efficiency is a result of low resolution and simplified dynamics. The global-scale ocean circulation is reasonably well represented, as shown by [9], whereas feedbacks involving changes in atmospheric circulation, precipitation patterns or land-surface processes are relatively poorly represented or ignored. The model is described briefly in [5] and more fully in [6]. For completeness, we give a brief summary of the model dynamics below. Readers interested only in the coupled problem may skip to the next section.

2.2.1. Ocean

The horizontal component $\mathbf{u}_\mathrm{h}$ of the oceanic velocity vector $\mathbf{u}$ satisfies the equation:

$$\mathbf{f} \times \mathbf{u}_\mathrm{h} = -\nabla_\mathrm{h} p - \lambda \mathbf{u}_\mathrm{h} + \frac{\partial}{\partial z}\boldsymbol{\tau}, \tag{19}$$

which expresses geostrophic balance between the Coriolis force due to the vertical component, $\mathbf{f}$, of the earth's

Table 1
Economy parameters.

Parameter	Notation	Value
Number of years in a period	d	10
Depreciation rate on capital per year	δ	0.1
Utility function coefficient	α	1
Initial rate of social time preference per year	r_1	0.03
Decline rate of social time preference per year	r_2	0.0025719
1990 world population (millions)	L_0	5,632.7
Life rate of population per period	g_{L_0}	0.7072
Decline rate of population growth per period	g_δ	0.222
Initial rate of technology change per period	g_{A_0}	0.55
Decline rate of technology change per period	g_δ	0.0016
Emission from deforestation (b.t.c.[a] per period)	ET_0	11.28
Decline rate of deforestation per period	g_{ET}	0.105

[a] b.t.c.: billion tons of carbon.

rotation vector and the horizontal component of the gradient of pressure p, modified by a frictional drag term with coefficient λ. τ is the wind stress, which acts only at the surface. The vertical velocity is derived from the mass conservation relation:

$$\nabla.\mathbf{u} = 0, \tag{20}$$

while the momentum balance in the vertical (z) direction:

$$\frac{\partial p}{\partial z} = -g\rho_o(T_o, S), \tag{21}$$

relates p (through the gravitational acceleration g) to the ocean density ρ_o, which, in turn, is a polynomial function of the oceanic temperature T_o and salinity S. These are governed by the generic advection–diffusion equation:

$$\frac{\partial X}{\partial t} + \nabla.(\mathbf{u}X) = \nabla.(\kappa\nabla X) + \mathcal{C}, \tag{22}$$

where $X = T_o$ or S. Note that throughout this section, the time t is a *continuous* variable. The diffusivity κ is a non-diagonal tensor with large components, representing eddy-induced advection and mixing, resolved along directions (which vary in time and space) parallel to constant density surfaces plus a very small component in the vertical direction, which causes mixing across density surfaces. The convective adjustment term, $\mathcal{C}$, mixes T_o and S vertically to ensure gravitational stability (light fluid above dense).

2.2.2. Atmosphere

The dynamic variables in the one-layer atmosphere are surface air temperature T_a and surface specific humidity q (note that the temperature values used as coupling variables are the global averages of T_a for the relevant periods). The governing equations are

$$\rho_a h_T C_{pa}\left(\frac{\partial T_a}{\partial t} + \nabla.(\beta_T\mathbf{u}T_a) - \nabla.(\kappa_T\nabla T_a)\right) = Q_{SW}C_A + Q_{LW} - Q_{PLW} + Q_{SH} + Q_{LH}, \tag{23}$$

$$\rho_a h_q\left(\frac{\partial q}{\partial t} + \nabla.(\beta_q\mathbf{u}q) - \nabla.(\kappa_q\nabla q)\right) = \rho_{oc}(\mathcal{E} - P) \tag{24}$$

where h_T and h_q are atmospheric boundary layer depths for heat and moisture respectively, whereas κ_T and κ_q are eddy diffusivities. κ_T is given by a simple exponential function, whereas κ_q is constant. $\mathcal{E}$ is the evaporation or sublimation rate, P is the precipitation rate and ρ_a and ρ_{oc} are constant representative densities for air and water, respectively. C_{pa} is the specific heat of air at constant pressure. The parameters β_T, β_q allow for a linear scaling of the advective transport term, which assumes a fixed, observationally derived velocity field $\mathbf{u}$. The constant C_A parameterizes the absorption by water vapour, dust, ozone, clouds, etc. of incoming short-wave solar radiation Q_{SW}. Q_{LW} is the long-wave imbalance at the surface. Q_{PLW} is the planetary long-wave radiation to space, given by a polynomial function, cubic in temperature T_a and quadratic in relative humidity q/q_s, where q_s is the saturation specific humidity: exponential in the surface temperature. For anthropogenically forced experiments, a greenhouse warming term is added to Q_{PLW}, which is proportional to the log of the ratio of carbon dioxide (CO_2) concentration compared to a pre-industrial reference value. The sensible heat flux Q_{SH} depends on the air-surface temperature difference and the surface wind speed (derived from ocean wind-stress data), and the latent heat release Q_{LH} is proportional to the precipitation rate P. Precipitated moisture is removed instantaneously so that the relative humidity never exceeds a fixed threshold value.

2.2.3. Sea ice

The fraction of the ocean surface covered by sea ice in any given region is denoted by A. Dynamical equations are solved for A and for the average height H of sea ice. In addition, a diagnostic equation is solved for the surface temperature T_i of the ice. Thermodynamic growth or decay of sea ice in the model depends on the net heat flux into the ice from the ocean and atmosphere. Sea-ice dynamics consist of advection by the surface current $\mathbf{u}_\mathrm{h}$ and Laplacian diffusion with constant coefficient κ_{hi}.

The growth rate G_i of sea-ice height in the ice-covered ocean fraction is

$$G_i = \frac{Q_b - Q_t}{\rho_i L_f} - \mathcal{E}\frac{\rho_{oc}}{\rho_i}, \tag{25}$$

where L_f is the latent heat of fusion of ice, ρ_i is its (constant) density, Q_b is the flux of heat from sea ice to ocean and Q_t is the flux of heat from atmosphere to sea ice. In the open-ocean fraction, we take $-Q_b$ to be the largest possible heat flux out of the ocean. Thus, if the ocean-to-atmosphere heat flux is greater than this, the deficit leads to ice growth in the open water fraction. The growth rate of sea ice in the open-ocean fraction is therefore

$$G_o = \max\left(0, \frac{Q_b - Q_{to}}{\rho_i L_f}\right), \tag{26}$$

where Q_{to} is the heat flux from atmosphere to ocean. The rate of change of the average sea-ice height, H, is then given by

$$\frac{\partial H}{\partial t} + \nabla.(\mathbf{u}_\mathrm{h}H) - \kappa_{hi}\nabla_h^2 H = AG_i + (1-A)G_o, \tag{27}$$

where κ_{hi} is a horizontal diffusivity. The rate of change of sea-ice area A is given by

$$\frac{\partial A}{\partial t} + \nabla.(\mathbf{u}_\mathrm{h}A) - \kappa_{hi}\nabla_h^2 A = \max\left(0, (1-A)\frac{G_o}{H_0}\right) + \min\left(0, AG_i\frac{A}{2H}\right). \tag{28}$$

The first term on the right-hand side parameterizes the possible growth of ice over open water, where H_0 is a minimum resolved sea-ice height. The second term parameterizes the melting of sea ice.

2.2.4. Solution method

Equations are discretized in finite-difference form on a spherical grid with 36 × 36 equal-area cells in the horizontal. The ocean component has eight vertical levels. The dynamic equations for T_o, S, T_a, q, H and A are integrated forward in time from a uniform initial state for around 5,500 years until an almost exactly steady state is reached. This can be taken to represent the pre-industrial climate. The model is then integrated forward with observed atmospheric CO_2 concentrations from 1795 to 1995 to produce an initial condition for the coupled runs.

2.2.5. Carbon cycle

The model carbon cycle could be closed by the inclusion of ocean biogeochemistry and a land-surface model without significant loss in efficiency. Such a coupled model is under development through the UK GENIE project, but here, for simplicity, we use the carbon-cycle dynamics of the DICE model.

The DICE carbon-cycle module consists of three linked reservoirs: the atmosphere, the upper ocean and biosphere combined and the deep ocean. The CO_2 accumulation and transportation is represented by a linear model. The basic structure is the following: emissions are added directly to the atmosphere, which communicates with the upper ocean-biosphere reservoir only. The upper ocean-biosphere also exchanges carbon with the deep ocean. The carbon cycle is assumed to be in equilibrium at the start of the coupled simulations. The transfer coefficients of the linear model are calibrated for a concentration of two times pre-industrial levels. The reference model is the Bern carbon-cycle model [14]. A full description of the carbon-cycle module is available in chapter 3 of [18].

3. The reduced-order optimisation problem

In this section, we define a reduced-order optimisation problem that involves only the coupling variables $\tilde{E}_{up}$ and $\tilde{T}_{lo}$, which are used to exchange information between the economic sub-model and the climate sub-model (the term "reduced order" refers to the fact that only these variables are involved). Recall that $\tilde{E}_{up} = (E_{up}(t) : t \in \mathcal{T} - \{t_{\max}\})$ and $\tilde{T}_{lo} = (T_{lo}(t) : t \in \mathcal{T})$ are the bounds on emissions and temperature change that are imposed in the economic model written in compact form in Eqs. (18a)–(18d). Indeed, the emission bounds provide a global emission path that will drive the climate model, whereas the temperature changes observed in the climate simulation will impose lower bounds on the temperature change used in the damage assessment in the economic model.

This reduced-order problem will be amenable to solution via an oracle-based optimisation (OBO) technique that we shall describe shortly. It will be convenient to denote by $X = (\tilde{E}_{up}, \tilde{T}_{lo}) \in \mathbb{R}^n$ the coupling variables, which represent the anthropogenic carbon emissions $\tilde{E}_{up}$ and the temperature changes $\tilde{T}_{lo}$.

The coupled optimisation problem for the integrated model is represented as the maximization of an objective function $U(X)$, which values the global utility of the world over the planning horizon $\mathcal{T}$, subject to $\Theta(X) \leq 0$, which represents a set of constraints related to climate change. More precisely

$$\max_{X \in \mathbb{R}^n} \{U(X) \mid (X) \leq 0\}, \tag{29}$$

where $U(X)$ is the optimum value for the economy model Eqs. (18a)–(18d) and $\Theta(X)$ is an impact function that controls the economic impact on climate defined as follows:

$$\Theta(X) = \phi(\tilde{E}_{up}) - \tilde{T}_{lo}, \tag{30}$$

where ϕ is the temperature change path computed by the climate oracle given the emission path $\tilde{E}_{up}$.

The optimum in (29) is denoted U^*, and the associated solution is X^*. To solve the problem, we use an oracle-based method, namely, the Proximal-ACCPM algorithm described in [20]. In this method, at each iteration, given a point $X^k \in \mathbb{R}^n$ generated by the Proximal-ACCPM algorithm, the oracle computes optimality cuts and feasibility cuts and a lower bound for the optimal value. Referring to the two-oracle structure portrayed in Figure 1, when optimality cuts are required, it is the economy oracle that is consulted, whereas feasibility cuts are obtained with information from the climate oracle. The cuts generated give an outer approximation of a so-called localization set in which the optimal solution lies. This localization is defined more precisely below. The method is guaranteed to converge with a relatively low number of queries if it deals with a convex optimisation problem. In our case, this means that the function $U(X)$ should be concave, and the function $\Theta(X)$ should be convex. We now discuss these assumptions.

3.1. Convexity

$U(X)$ is the optimal value of the economic model described in Section 2.1 subject to emissions and temperature constraints represented by $(\tilde{E}_{sup}, \tilde{T}_{lo})$ and summarized by X. The utility function, Eq. (2), is a concave function. The production function in Eq. (13) is concave. The state dynamics, represented by the capital accumulation Eq. (15), is linear. The value function $U(X)$ is therefore concave by construction [5].

The convexity of $\Theta(X)$ is more difficult to prove. The temperature change path $\phi(\tilde{E}_{up})$ computed by the climate model, which enters in the definition of $\Theta(X)$, is the result of a complex and highly non-linear process. There is no easy way to guarantee that this function is convex.

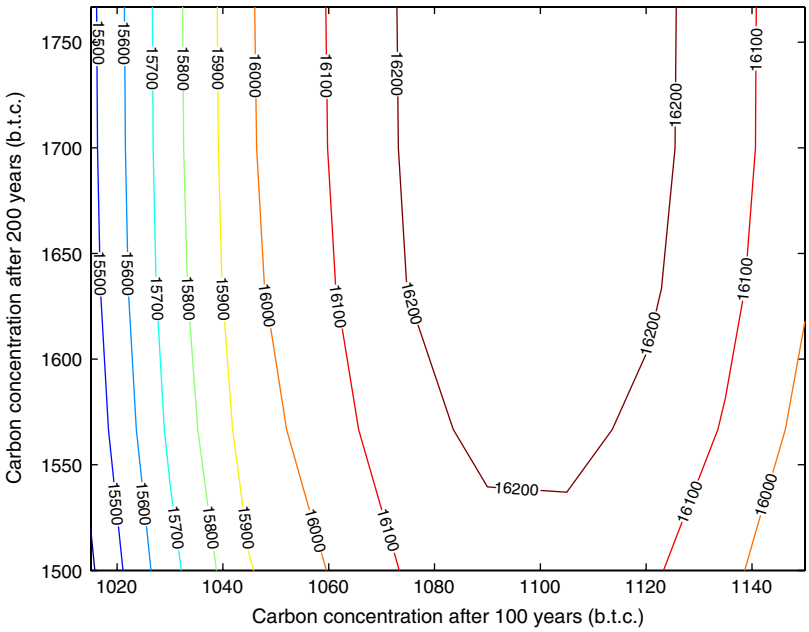

Figure 2. Contour plot of the reduced-order problem.

Furthermore, in contrast to the earlier study (in [5]) where the climate function returned only one value, here, the function $\Theta(X)$ returns a path of values. We therefore have to content ourselves with an "empirical" observation of convex behaviour of $\Theta(X)$ in the domain of interest of X. Note that convex behaviour of $\Theta(X)$ is in line with a basic understanding of the climate system, in which increased emissions in any period would lead to non-negative change in global average temperature for all future times.

Some experiments have been carried out to assess the shape of the reduced-order model. We choose a four-component coupling variable $X = (E_{100}, E_{200}, T_{100}, T_{200})$ where two milestones, at 100 and 200 years, have been chosen. We select 1,000 points in a box domain for the value of the emissions E_{100} and E_{200}. Then we compute the associated concentrations and temperature change using the modules of the climate oracle. Finally, we solve the reduced problem with fixed X. We thus obtain the global welfare for each of these points. Figure 2 represents the resulting distribution of global welfare as a function of the carbon concentrations after 100 and 200 years. The function appears convex with a more planar region at high values of concentration.

Although this empirical verification looks encouraging, we cannot rule out some non-convex regions in the domain of $\Theta(X)$. Therefore, it is necessary to implement a back-tracking procedure to restart the optimisation process when local non-convexity causes the algorithm to stall.

3.2. The Proximal-ACCPM Algorithm

In this section, we recall the basic features of the OBO procedure as described in [2]. The convex optimisation problem (29) belongs to the class of problems that can be solved through an OBO technique: the hypograph of $U(X)$ (defined as $\{(X,z) \in \mathbb{R}^{n+1} \mid z \leq U(X)\}$) and the feasible set can be delineated by a polyhedral outer approximation. We use the Proximal-ACCPM algorithm [20], an enhanced interior point cutting plane method for convex optimisation problems, to implement the OBO approach. The algorithm proceeds as follows. Given a point $\bar{X}^k$, the procedure calls the oracle, which tests if this point lies in the feasible set. If it does, the oracle returns an optimality cut for $U(X)$ (to be defined shortly in Section 3.3). If not, the oracle returns a set of feasibility cuts for either the domain of $\Theta(X)$ (see Section 3.4) or the domain of $U(X)$ (see Section 3.5). The intersection of the half-spaces circumscribed by the cuts forms the localization set, denoted $\mathcal{L}^k$. This polyhedral set corresponds to a superset of the linear outer approximation of the hypograph of U and contains the optimal solution X^* and the associated objective value $U^* = z^*$. Proximal-ACCPM, specifically its query point generator module, chooses the next point $\bar{X}^{k+1}$ as the analytic centre of $\mathcal{L}^k$ (see [2] for a definition of this concept and the Newton procedure to calculate it). The procedure calls the oracle with the new point and generates one or several new cuts. A new localization set $\mathcal{L}^{k+1}$ is thus obtained as follows:

$$\mathcal{L}^{k+1} = \mathcal{L}^k \cap \{(X,z) \mid \theta_l \leq z \leq U(\bar{X}^k), \\ X \in \{O^k \cup F_U^k \cup F_\Theta^k\}\}, \tag{31}$$

with $\mathcal{L}^0 = \{(X,z) \in \mathbb{R}^{n+1}\}$ and where given the iteration k, we define: θ_l the highest lower bound obtained during the process; O^k the half-space defined by the optimality cut if it exists, $\emptyset$ otherwise; F_U^k the intersection of the half-spaces defined by the feasibility cuts for the domain of U if they exist, $\emptyset$ otherwise; and F_Θ^k the intersection of the half-spaces defined by the feasibility cuts for the domain of Θ if

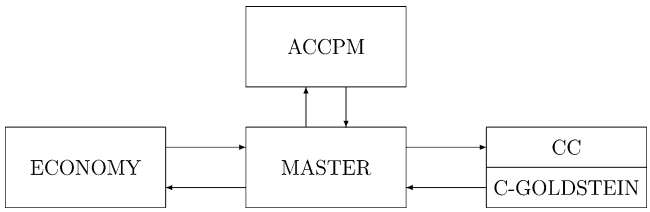

Figure 3. GOLDICE structure: arrows show physical data exchange between sub-programs.

they exist, $\emptyset$ otherwise. Expression (31) defines a set that contains the optimal pair (X^*, U^*) and which shrinks at each iteration. When the localization set is small enough, it defines the optimal pair (X^*, U^*) within the prescribed tolerance level and the procedure ends.

We can thus summarize our implementation of Proximal-ACCPM as follows.

3.2.1. Initialization

First, choose a starting point $\bar{X}^0 = (E^0, T^0)$. Generally, we choose E^0 as the optimal carbon emission pathway of DICE-99 and T^0 as the associated temperature change pathway computed by C-GOLDSTEIN. Then, the bounds are initialized as $\theta_l = -\infty$ et $\theta_u = +\infty$, and an optimality tolerance ϵ is defined.

3.2.2. Proximal-ACCPM iteration k

1. Choose the $\bar{X}^k$ as the analytic centre of the localization set $\mathcal{L}^k$ and an associated upper bound $\bar{\theta}_u$.
2. Call the oracle at $\bar{X}^k$
   (a) Compute the value of $\Theta(\bar{X}^k)$.
   (b) If $\Theta(\bar{X}^k) > 0$, then generate a feasibility cut for the domain of $\Theta(X)$.
   (c) If $\Theta(\bar{X}^k) \leq 0$, then solve the problem $U(\bar{X}^k)$.
      i. If $U(\bar{X}^k)$ is infeasible, then generate a feasibility cut for the domain of $U(X)$.
      ii. If $U(\bar{X}^k)$ is feasible, then generate an optimality cut. $\theta_l = \max(\mathrm{U}(\mathbf{X}^{\mathrm{k}}), \theta_{\mathrm{l}})$.
   (d) Return the generated cuts and the lower bound.
3. Update the upper bound: $\theta_u = \min(\theta_{\mathrm{u}}, \theta_{\mathrm{u}})$.
4. If $\theta_u - \theta_l \leq \epsilon$, stop the procedure.
5. Update $\mathcal{L}^{k+1}$.

The following sections focus on the calculation of the cuts inside the oracles. From now on, the scalar product of the vectors u and v will be denoted by $\langle u, v \rangle$.

3.3. Generation of an optimality cut for $U(X)$

When $\bar{X} = (\tilde{E}_{up}, \tilde{T}_{lo})$ belongs to the domain of the reduced-order problem (29), Proximal-ACCPM generates an optimality cut. An optimality cut for $U(X)$ is a half-space defined by a supporting plane to the hypograph of the function $U(X)$ at the given point $\bar{X}$. It takes the following form

$$\{X \in \mathbb{R}^n \mid U(\bar{X}) + \langle \xi, (X - \bar{X}) \rangle \geq U(X)\}, \tag{32}$$

where $\xi \in \partial U(\bar{X})$[1] is a supergradient of the function U at $\bar{X}$. As defined in Section 2.1, $U(\bar{X})$ is the optimal value of the objective function in the problem (18a)–(18d). The Lagrangian form of this problem at the optimum is

$$f(\tilde{E}^*, \tilde{T}^*, \upsilon^*) - \langle w, \psi(\tilde{E}^*, \tilde{T}^*, \upsilon^*) \rangle - \langle u_1, \tilde{E}^* - \tilde{E}_{up} \rangle - \langle u_2, \tilde{T}^* - \tilde{T}_{lo} \rangle \tag{33}$$

where w, u_1 and u_2 correspond to the optimal dual values of Eqs. (18b), (18c) and (18d), respectively. The supergradient is obtained from the dual variables, i.e. $\xi = (u_1, u_2)$.

3.4. Generation of the feasibility cut for $\Theta(X)$

A feasibility cut for $\Theta(X)$ defines a half-space E_0 that contains the feasibility set, which contains $X^* \in E_0$. This half-space is defined by the expression

$$\{X \in \mathbb{R}^n \mid \langle \nabla\Theta(\bar{X}), (X - \bar{X}) \rangle + \Theta(\bar{X}) \leq 0\}, \tag{34}$$

where $\nabla\Theta(\bar{X})$ is the Jacobian matrix of Θ at $\bar{X}$. Let p and q be the numbers of components of the subvectors $\bar{E}$ and $\bar{T}$, respectively. Using Eq. (30), the Jacobian matrix is $\nabla\Theta(\bar{X}) = (\nabla\phi(\bar{E}), -I)$, where I is the identity matrix with dimension q. The Jacobian matrix $\nabla\phi(\bar{E})$ can only be evaluated numerically by the climate oracle. We use a finite difference method to approximate it.

$$\nabla\phi_{ij}(\bar{E}) = \frac{\partial\phi_i}{\partial\bar{E}_j} \approx \frac{\phi_i(\bar{E} + \epsilon e_j) - \phi_i(\bar{E})}{\epsilon}, \quad i = 1, \ldots, q,\ j = 1, \ldots, p \tag{35}$$

[1] U is a non-differentiable concave function. Therefore, we must work with "supergradients" since the simple gradient $\nabla\bar{X}$ may not be well defined.

Table 2
GOLDICE components.

Name	Description	Call time
C-GOLDSTEIN	Climate model	5 min
ECONOMY	Economy growth	0.15 s
CC	Carbon cycle	∼
ACCPM	Search algorithm	0.05 s
MASTER	Director	∼

where $\epsilon > 0$ represents a perturbation in the carbon emission pathway and $e_j = (0, \ldots, 0, 1_i, 0, \ldots, 0)$. $\phi_i(\bar{E})$ is the temperature change pathway given the emissions $\bar{E}$. $\nabla\phi(\bar{E})$ is a matrix with p rows and q columns:

$$\nabla\phi(\bar{E}) = \begin{pmatrix} \nabla\phi_{11}(\bar{E}) & \cdots & \nabla\phi_{1p}(\bar{E}) \\ \vdots & \ddots & \vdots \\ \nabla\phi_{q1}(\bar{E}) & \cdots & \nabla\phi_{qp}(\bar{E}) \end{pmatrix}. \quad (36)$$

A column vector is obtained with a single climate simulation (i.e., a single run of C-GOLDSTEIN plus DICE carbon cycle): the first column of the matrix corresponds to the temperature change pathway given a perturbation of the carbon emissions in period 1, for the second column, the perturbation occurs in period 2 and so on. Therefore, we need $p + 1$ climate simulations to calculate the entire Jacobian matrix [one simulation is needed to obtain the vector $\phi_i(\bar{E})$]. The climate simulation is a dynamic process, so a perturbation in the carbon emission pathway should only affect the temperature changes of the following periods. The partial derivatives of the periods preceding the perturbation are therefore equal to zero. The Jacobian matrix can thus be rewritten in the following form:

$$\nabla\phi(\bar{E}) \approx \begin{pmatrix} \nabla\phi_{11}(\bar{E}) & 0 & 0 \\ \vdots & \ddots & 0 \\ \nabla\phi_{q1}(\bar{E}) & \cdots & \nabla\phi_{qp}(\bar{E}) \end{pmatrix}. \quad (37)$$

The C-GOLDSTEIN and DICE carbon-cycle models have the capability to "warm start" in beginning the simulation at a given "state of the world," which consists in a set of variables and values that describe their view of the world at a given moment. The "states of the world" are recorded during the computation of $\phi(\bar{E})$, and in computing the Jacobian matrix, we can reduce the time horizon of the simulation for each new computed column vector. This technique reduces by almost a factor of 2 the total time of calculation of the Jacobian matrix. We may envisage more significant gains by implementing automatic differentiation within the climate model.

3.5. Generation of feasibility cuts for the domain of U

In practice, it is not necessary to generate feasibility cuts for the domain of U. It is easy to find a set of values for $\tilde{E}_{up}$ and $\tilde{T}_{lo}$ that are of interest and make U feasible. We denote by D_U this subset of the domain of the function U. From Eq. (13), we deduce that the lowest values for $\tilde{E}_{up}$ are the exogenous deforestation emissions ET, defined by $(ET(t) : t \in \mathcal{T} - \{t_{\max}\})$. Conversely, experience suggests

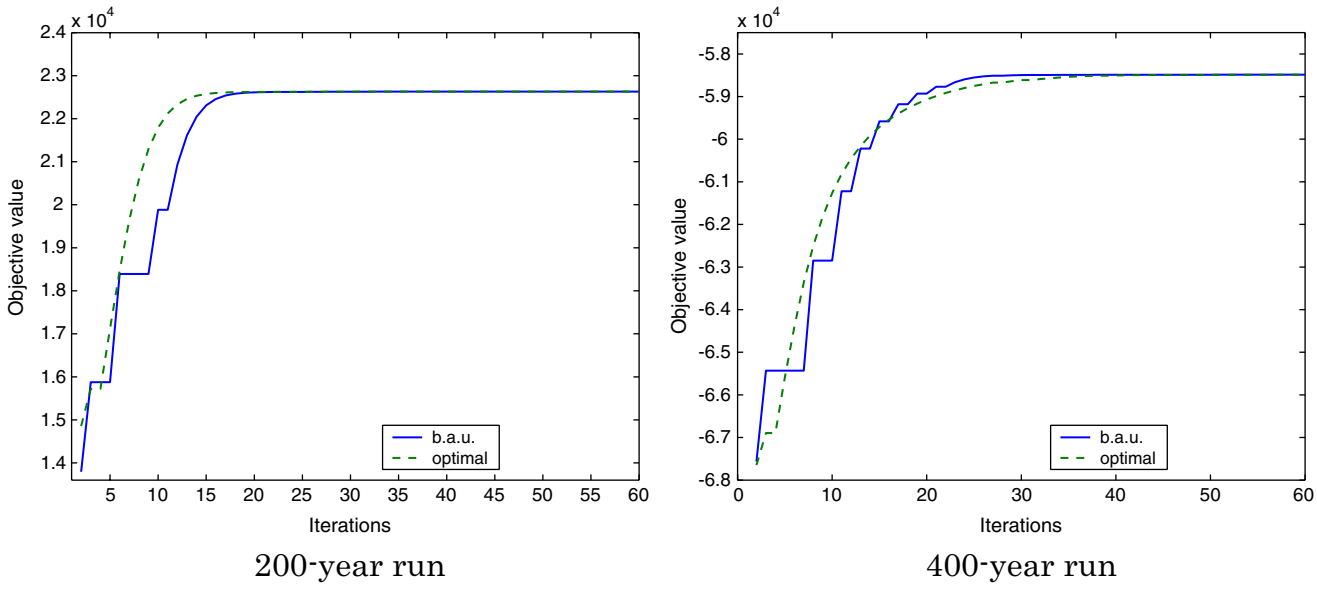

Figure 4. Convergence of the objective values (the discounted global welfare) for GOLDICE for two different run lengths and two different starting points.

Table 3
Total discounted welfare values for DICE-99 and GOLDICE.

	200-year run	400-year run
DICE-99	22,570.20	−58,647.20
GOLDICE	22,630.46	−58,410.55

that +10°C represents a sufficient upper bound for the temperature change. We thus define

$$D_U = \{(\tilde{E}_{up}, \tilde{T}_{lo}) \mid \tilde{E}_{up} \in [ET; +\infty], \quad \tilde{T}_{lo} \in [-\infty; 10]\}. \tag{38}$$

Although feasibility cuts are not required for the domain of U in our case, they could readily be calculated in the following way. Let $\bar{X}$ be a point that does not belong to the domain of U. We need to solve the following auxiliary problem obtained from Eqs. (18a)–(18d) by introducing artificial variables in the constraints and replacing the objective $U(X)$ by the maximum value of the artificial variables.

$$\min \iota = \max(\iota_1, \iota_2) \tag{39a}$$

$$\text{s.t.} \quad \psi(\tilde{E}, \tilde{T}, \upsilon) \leq 0, \tag{39b}$$

$$\tilde{E} - E_{up} - \iota_1 \leq 0, \tag{39c}$$

$$\tilde{T} - T_{lo} + \iota_2 \geq 0, \tag{39d}$$

$$\iota_1, \iota_2 \geq 0. \tag{39e}$$

We then introduce the feasibility cut:

$$\{X \in \mathbb{R}^n \mid \langle \gamma, (X - \bar{X}) \rangle + \iota^* \leq 0\}, \tag{40}$$

where γ is the dual value associated to Eqs. (39c) and (39d) when the optimal value ι^* is obtained.

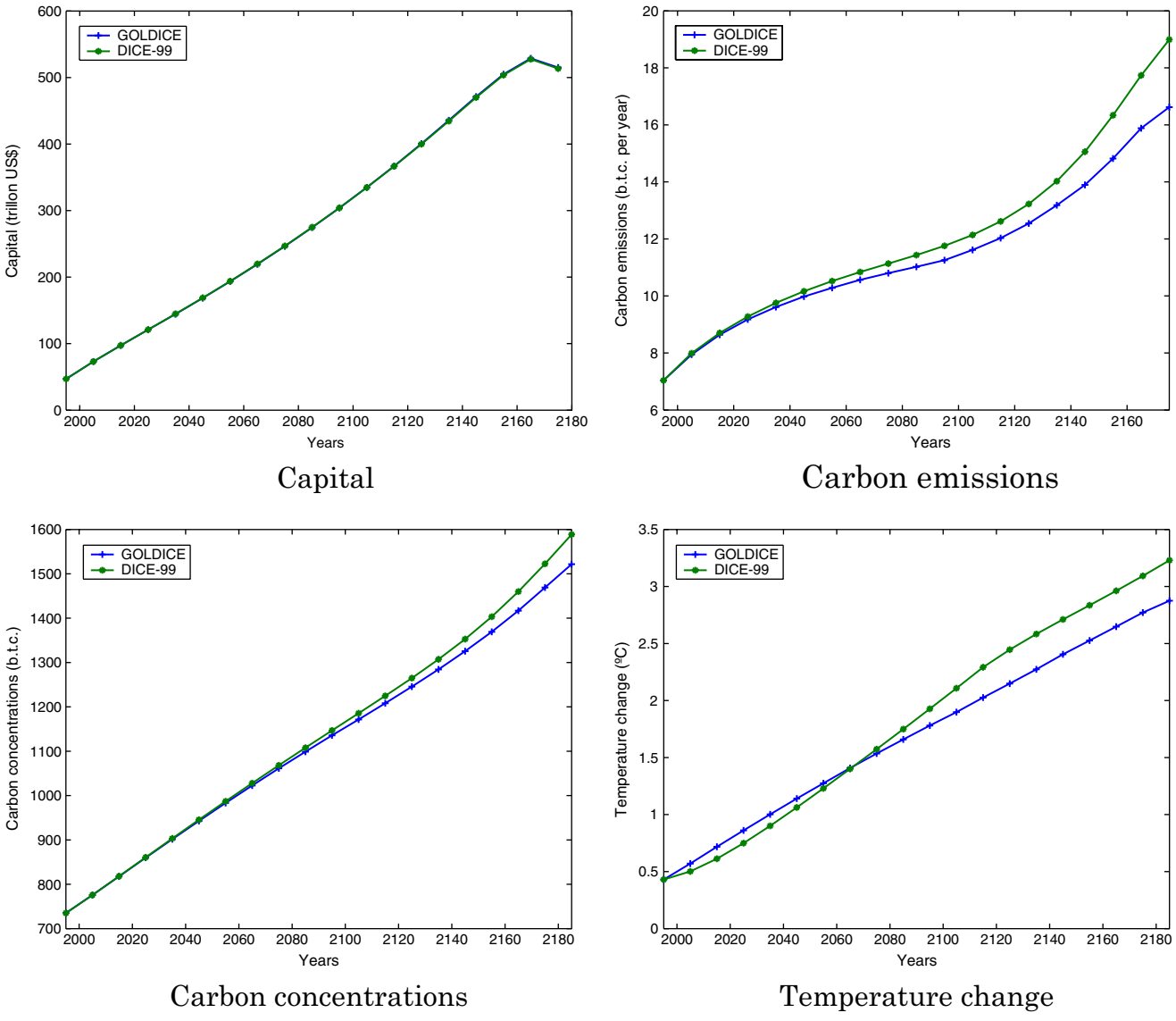

Figure 5. Optimal policies for DICE-99 and GOLDICE-200 with a 200-year run.

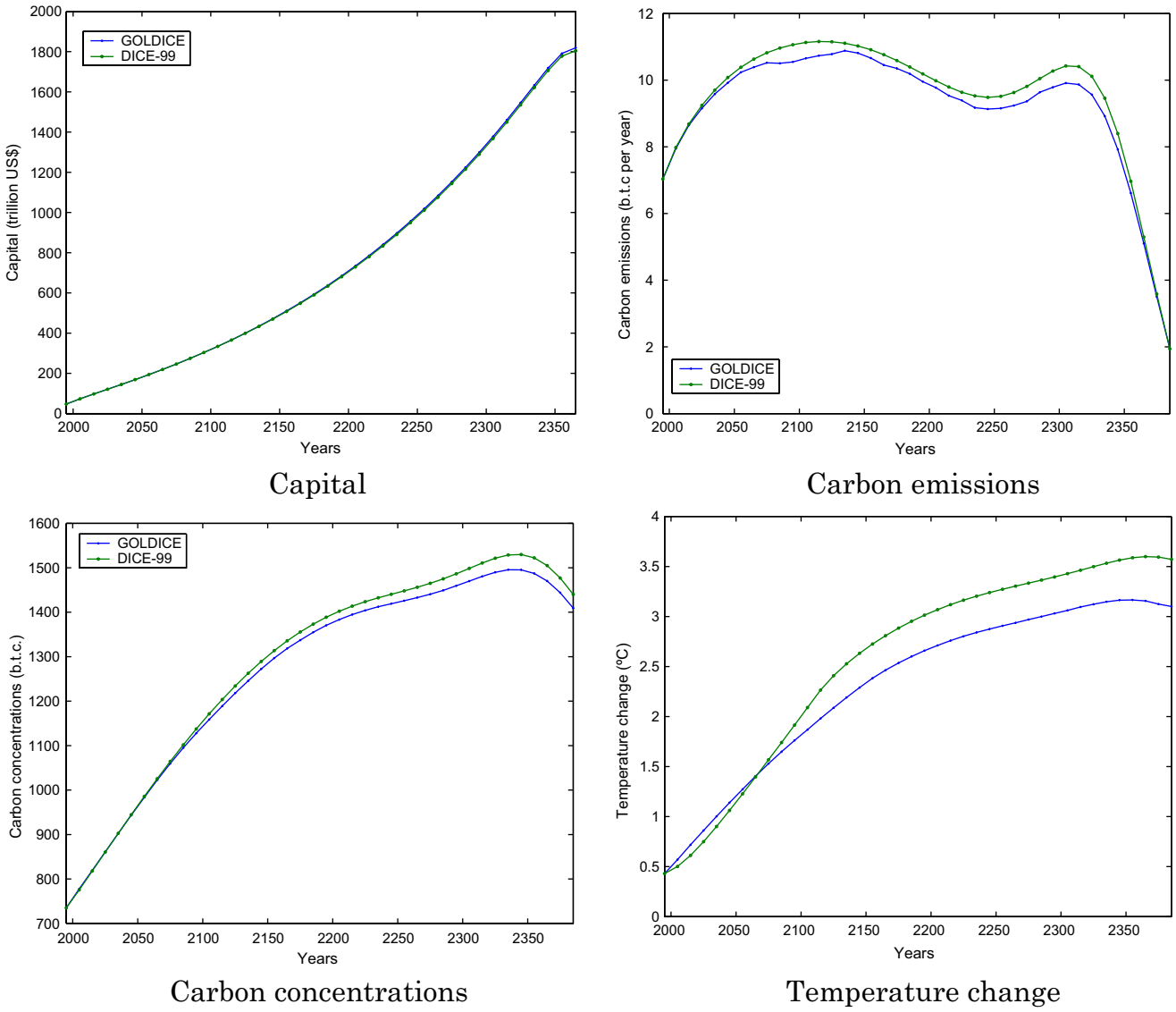

Figure 6. Optimal policies for DICE-99 and GOLDICE-400 with a 400-year run.

4. Implementation issues

4.1. Technical details

The coupled model was implemented on a Linux machine with 2×2.4 GHz processors. An effort was made to create a flexible and expansible structure composed of independent modules. The introduction of a new module or the replacement of an existing module is relatively easy. Each module has a directory dedicated to the inputs, the outputs and the executable code. The economic growth module and the carbon-cycle module are written in GAMS. C-GOLDSTEIN is written in FORTRAN. Proximal-ACCPM is written in the MATLAB language. The master program is also written in MATLAB. Its role is to initialize Proximal-ACCPM and to exchange information with each module. The MATLAB language provides tools to create and read formatted text files but also powerful tools for building mathematical objects needed by Proximal-ACCPM. Figure 3 shows an overview of the GOLDICE structure and the communications between the parts of the model. Table 2 reports details of the nature of these parts, the inputs and outputs they accept and the time they need to run. Currently, the communication between the different parts is achieved by reading and writing files in a dedicated directory, but the program should be easily adaptable to an XML-based description and encapsulation of data.

4.2. Numerical results

We now compare the results of GOLDICE with those of DICE-99. Two different runs have been made to test the method. We compute the optimal policy for a 200-year (GOLDICE-200) and a 400-year (GOLDICE-400) run, and we compare the results with those obtained with DICE-99 running along a similar number of periods.

Figure 4 plots the values of objective function of the reduced-order problem for the two runs and for two different

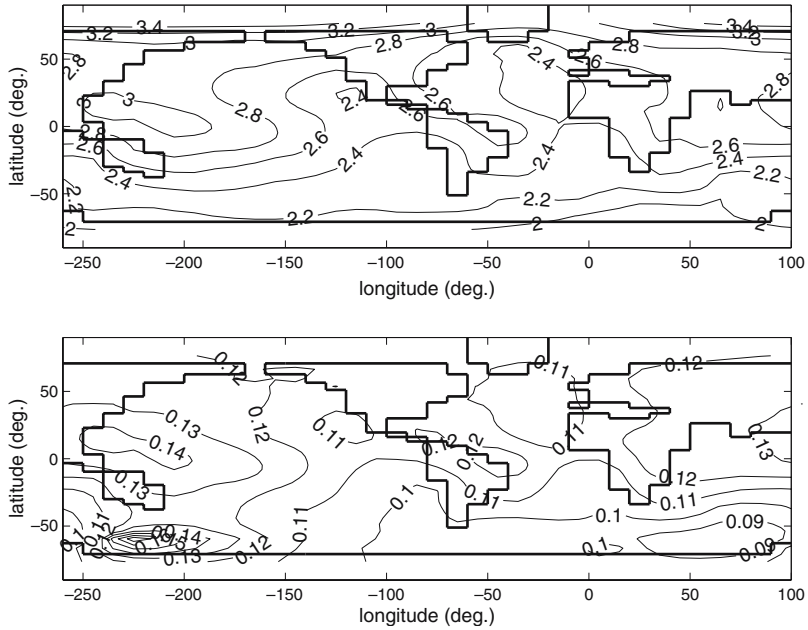

Figure 7. Increase in surface air temperature at the end of the run in the GOLDICE-200 solution in degree Celsius (upper panel), and the difference between this state and the corresponding state forced by DICE emissions (lower panel).

starting points: *optimal*, which is the DICE-99 optimal solution, and *b.a.u.*, which is the DICE-99 optimal solution without emission abatement. The graphs show the convergence of the method for the two cases. The method goes towards a solution close to optimality in a relatively small number of iterations. GOLDICE-400 is much harder and more time consuming to solve: the computation of a gradient corresponds to several successive calls to C-GOLDSTEIN, and the time of computation increases with the augmentation of the time horizon. A typical GOLDICE-400 gradient computation costs 1.5 h of computation against 30 min for GOLDICE-200. The generation of a feasibility cut is thus very costly. Beginning with a good starting point reduces dramatically the number of feasibility cuts and thus the total time taken to solve the problem. The total discounted welfare values obtained with the two models are shown in Table 3; we observe relatively close values. Figures 5 and 6 report the behaviour of the key variables of GOLDICE and DICE-99 for the 200- and the 400-year run, respectively. The figures reproduce only the capital accumulation path because the differences between GOLDICE and DICE-99 are small for the other economic variables. More differences appear in the coupling variables: emissions and temperature change. GOLDICE-200 results are a little bit more restrictive on the economy. The optimal emissions path is 2 Gt per year lower at the end of 200 years for GOLDICE-200 in comparison with DICE-99. Temperature change is equal to 2.8°C after 200 years, which is 0.4°C colder than DICE-99. We observe similar results with GOLDICE-400. Figure 5 plots the temperature changes from C-GOLDSTEIN for an optimal carbon path of DICE-99 over 200 years versus temperature changes computed by DICE-99. The C-GOLDSTEIN curve is closer to a linear trend than the DICE-99 curve, but the distance between the two curves is relatively small. This suggests that the basic climate sensitivity of DICE-99 is similar to that of C-GOLDSTEIN, and that no significantly non-linear changes occur, such as major reorganization of the ocean circulation. In both models, the basic atmospheric sensitivity to changes in radiative forcing via CO_2 changes corresponds to a single, adjustable parameter value. The key climate sensitivity parameter of the DICE-99 module gives a warming of 2.9°C associated with a doubling of the carbon concentration in the atmosphere (the same value was found for C-GOLDSTEIN in [9]), which is 0.4°C warmer than the average estimated value suggested by the IPCC, although this value is not well constrained by data or numerical models. The added value of using an intermediate complexity model such as C-GOLDSTEIN is the large amount of extra information on climate variables, e.g. the spatial distribution of air temperature and the ocean circulation. Figure 7 shows the surface air temperature increase at the end of the run after 200 years in the final GOLDICE-200 solution, and the difference between this and the corresponding temperature field when the climate model is forced by the DICE emissions. The pattern of global warming shows the usual polar and continental amplification, with weaker warming in the North Atlantic and southern ocean regions. The DICE solution is warmer by 0.1–0.18°C, with a peak in the southern ocean related to temporal changes in convection close to the Antarctic shelf. Figure 8 shows the overturning stream function in the Atlantic (a potential function for the integrated mass transport in a vertical-latitude plane – a representation of the thermohaline circulation). The top plot shows the initial overturning, the middle plot, the

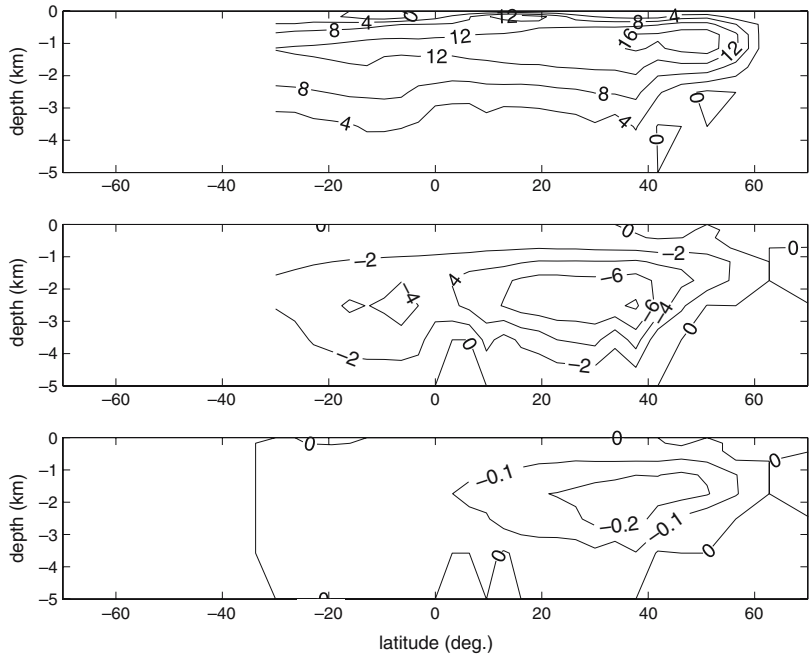

Figure 8. Overturning stream functions in the Atlantic basin in Sv (1 Sv $= 10^6$ m^3s^{-1}). Upper panel: initial state representing 1995 conditions; middle panel: change in overturning at the end of the run in the GOLDICE-200 solution; lower panel: difference between the GOLDICE and DICE emission-forced solutions.

change in overturning in the final state, relative to the initial state, and the lower plot of the difference between GOLDICE and DICE solutions. Warming leads to a reduction in the maximum overturning from 18 to 17 Sv (1 Sv $= 10^6$ m^3s^{-1}) accompanied by a reduction in the depth of the overturning cell, the changes being slightly more pronounced in the DICE-forced solution.

5. Conclusion

In this paper, we have shown how to integrate a time-dependent (simulation) climate model within an optimisation framework. We have succeeded in exchanging the DICE-99 temperature module for an intermediate complexity 3-D climate model, thus giving a climate representation within the globally aggregated economic growth model, which is more rationally derived from fundamental physical principles and thus able to respond in a more faithful way to calculated changes in emissions.

Although the results of the present coupled model tend to show that DICE-99 was already capturing much of the information on possible globally averaged temperature change, the proposed coupling technique provides interesting avenues for further IAM developments. In principle, our climate model can provide more information than the globally averaged temperature change. It can also supply regionalized information on temperature, humidity and precipitation change. Changes in the Atlantic thermohaline circulation, for example, could be directly calculated and used in a damage function.

The incorporation of physically based climate models lends considerable credibility to the results of an integrated assessment modelling exercise compared to the use of simple temperature change functions as in the original DICE model. The full potential of IAMs using more elaborate climate models, however, will only be realized when the extra information they can provide is fully utilized. Future research will focus on replacing the economy model with a more encompassing one, like, for example, the ICEMODE model of ICLIPS or the ETA-MACRO model of ICLIPS. This coupling would add a regional scale for the economy and will permit the use of a more representative regionalized damage function. A further important improvement to the present model will be the incorporation of a consistent carbon-cycle representation within the climate model.

Acknowledgements

The authors thank J.P. Vial, F. Babonneau and C. Beltran for their assistance and guidance in the implementation of Proximal-ACCPM. This work has been supported by the SNSF-NCCR Climate grant.

References

[1] J. Alcamo, M. Krol and R. Leemans, Stabilizing greenhouse gases: Global and regional consequences. Technical report, Bilthoven, The Netherlands: National Institute of Public Health and the Environment (RIVM) (1995).

[2] F. Baboneau, C. Beltran, A.B. Haurie, C. Tadonki and J.-Ph. Vial, Proximal-ACCPM: a versatile oracle based optimization method, to appear in the special issue of Computational Management Science on Advances in computational economics, finance and management science, B. Rustim, Kluwer.

[3] D.A. Carlson, A. Haurie, J.-P. Vial and D.S. Zachary, Large-scale convex optimization method for air quality policy assessment. Automatica 40(3) (2004) 385–395, March.

[4] S.H. Dowlatabadi, Climate change thresholds and guardrails for emissions (editorial). Clim. Change 3/4 (1999) 297–301.

[5] L. Drouet, C. Beltran, N.R. Edwards, A.B. Haurie, J.-P. Vial and D.S. Zachary, An oracle method to couple climate and economic dynamics, in: *Coupling climate and economic dynamics*, eds. A. Haurie and L. Viguier (Kluwer, Dordrecht, The Netherlands, 2005).

[6] N.R. Edwards and R. Marsh, Uncertainties due to transport-parameter sensitivity in an efficient 3-D ocean-climate model. Clim. Dyn. 24 (2005) 415–433.

[7] J.-L. Goffin, A. Haurie and J.-P. Vial, Decomposition and non-differentiable optimization with the projective algorithm. Manage. Sci. 38 (1992) 284–302.

[8] C. Gordon, C. Cooper, C.A. Senior, H. Banks, J.M. Gregory, T.C. Johns , J.F.B Mitchell and R.A. Wood, The simulation of SST, sea-ice extents and ocean heat transports in a version of the Hadley Centre coupled model without flux adjustments. Clim. Dyn. 16 (2000) 147–168.

[9] J.C. Hargreaves, J.D. Annan, N.R. Edwards and R. Marsh, Climate forecasting using an intermediate complexity Earth System Model and the Ensemble Kalman Filter. Clim. Dyn. 23 (2004) 745–760.

[10] A. Haurie, Integrated assessment modeling for global climate change: An infinite horizon optimization viewpoint. Environ. Model. Assess. 8 (2003) 117–132.

[11] IPCC, *Climate Change 2001: The scientific basis*. IPCC Third Assessment Report (2001).

[12] C.C. Jaeger, M. Leimbach, C. Carraro, K. Hasselmann, J.C. Hourcade, A. Keeler and R. Klein, Integrated assessment modeling: Modules for cooperation. Working paper, FEEM Nota di Lavoro 53.2002, Fondacione Eni Enrico Mattei, Milan (2002).

[13] M. Jansenn, J. Totmans and K. Vrieze, Climate change: Optimization of response strategies. Int. Trans. Oper. Res. 2(1) (1995) 1–15.

[14] F. Joos, The atmospheric carbon dioxide perturbation. Europhys. News 27 (1996) 213–218.

[15] M. Leimbach and C. Jaeger, A modular approach to integrated assessment modeling. Environ. Model. Assess. 9 (2004) 207–220.

[16] A. Manne, R. Mendelsohn and R. Richels, A model for evaluating regional and global effects of GHG reduction policies. Energy Policy 1 (1995) 17–34.

[17] W.D. Nordhaus, Rolling the 'DICE': An optimal transition path for controlling greenhouse gases. Resour. Energy Econ. 15 (1993) 27–50.

[18] W.D. Nordhaus and J. Boyer, *Roll the DICE Again: Economic Models of Global Warming* (MIT Press, Cambridge, MA, 2000).

[19] E.A. Parson and K. Fisher-Vaden, Searching for integrated assessment: A preliminary investigation of methods, models, and projects in the integrated assessment of global climatic change. *Consortium for International Earth Science Information Network (CIESIN)* (1995).

[20] O. Péton and J.-P. Vial, A brief tutorial on ACCPM. Technical report, Logilab, University of Geneva (2001).

[21] J. Rotmans and M.B.A. Asselt, Integrated assessment: A growing child on its way to maturity. Clim. Change 34 (1996) 327–336.

[22] S.H. Schneider, Integrated assessment modeling of global climate change: Transparent rational tool for policymaking or opaque screen hiding value-laden assumptions? Environ. Model. Assess. 2(4) (1997) 229–248.

[23] F.L. Thot, T. Bruckner, H.-M. Fuessel, M. Leimbach and G. Petshel-Held, Integrated assessment of long-term climate policies: Part 1 – model presentation. Clim. Change 56 (2003) 37–56.

[24] R. Warren, A blueprint for integrated assessment of climate change. Technical report, Tyndall Centre. July (2002).

[25] A.J. Weaver, M. Eby, E.C. Wiebe, C.M. Bitz, P.B. Duffy, T.L. Ewen, A.F. Fanning, M.M. Holland, A. MacFayden, H.D. Matthews, K.J. Meissner, O. Saenko, A. Schmittner, H. Wang and M. Yoshimori, The UVic earth system climate model: Model description, climatology, and applications to past, present and future climates. Atmos.-Ocean 39 (2001) 361–428.

[26] T.M.L. Wigley, S.C.B. Raper, S. Smith and M. Hulme, The maggicc/scengen climate scenario generator: Version 2.4. Technical report, Climatic Research Unit, UEA, Norwich (2000).